63-1-3

GCA TECHNICAL REPORT 62-22-A

SATELLITE NAVIGATION BY TERRESTRIAL OCCULTATIONS OF STARS III: INTERFERENCE DUE TO BRIGHTNESS OF THE EARTH'S ATMOSPHERE

ROLLIN C. JONES ALI M. NAQVI

CONTRACT NO. AF33(616)-7413

AERONAUTICAL SYSTEMS DIVISION
AIR FORCE SYSTEMS COMMAND
UNITED STATES AIR FORCE
WRIGHT-PATTERSON AFB, OHIO

OCTOBER 1962

GEOPHYSICS CORPORATION OF AMERICA
BEDFORD, MASSACHUSETTS

GCA Technical Report 62-22-A

SATELLITE NAVIGATION BY TERRESTRIAL OCCULTATIONS OF STARS III:

INTERFERENCE DUE TO BRIGHTNESS OF THE EARTH'S ATMOSPHERE

Rollin C. Jones Ali M. Naqvi

Contract No. AF33(616)-7413

AERONAUTICAL SYSTEMS DIVISION
Air Force Systems Command
United States Air Force
Wright-Patterson AFB, Ohio

October 1962

GEOPHYSICS CORPORATION OF AMERICA
Bedford, Massachusetts

TABLE OF CONTENTS

FOREWORD

This study was undertaken as part of an investigation of navigation within the solar system by optical means. The objective of the investigation is to evaluate the suitability of various physical phenomena as sources of navigational information and to estimate the accuracy of navigational information obtained by various techniques. The work was supported under Contract No. AF 33(616)-7413 by the Navigational and Guidance Laboratory, Wright Air Development Division, Air Research and Development Command, United States Air Force.

The present report is one of a series of three entitled:

Satellite Navigation by Terrestrial Occultations of Stars

I. General Considerations Neglecting Atmospheric Refraction and Extinction by Ali M. Naqvi (GCA Tech. Report 62-18-A).

II. Considerations Relating to Refraction and Extinction by Ali M. Naqvi (GCA Tech. Report 62-21-A).

III. Interference Due to Brightness of Earth's Atmosphere by Rollin C. Jones and Ali M. Naqvi (GCA Tech. Report 62-22-A).

ABSTRACT

The radiance of the earth's atmosphere due to day and night airglow, noctilucent clouds, aurorae and Rayleigh scattering of the light from the sun and the moon is investigated and compared with the radiation received from some typical stars. Daytime observations of star occultations are ruled out on account of the very large radiance due to the scattering of sunlight. For nighttime observations the radiance due to night airglow and scattering of moonlight, especially near the full-moon phase, is likely to be troublesome.

SECTION 1

INTRODUCTION

Natural backgrounds may interfere with the detection process involved in monitoring a stellar signal required for satellite navigation. During vehicle trajectory varying radiative backgrounds may occur within the system's field-of-view depending on field-of-view, detectivity, look direction, spectral region and intensity levels of the phenomena encountered. Principal phenomena contributing to optical intensity and wavelength variations in background radiance observed by satellite-borne instrumentation are specifically attributed to:

(1) Solar radiation reflected by the earth's surface and various cloud layers including noctilucent clouds additive to Rayleigh and Mie solar scattering by the molecules and aerosols present in the atmosphere.

(2) Thermal radiation (present day or night) emitted by the earth, multiple cloud formations and the many molecular species that constitute the atmosphere.

(3) Nocturnal radiative sources such as stellar, auroral and airglow backgrounds, the latter originating from an emitting layer in the vicinity of 100 km.

Scattering of solar radiation by atmospheric aerosols and molecules is one contributing factor to radiance backgrounds in the visible and near infrared region (below 3 microns) during daylight hours. At night the background levels are less by 5 or 6 orders of magnitude in this spectral range and are influenced mainly by lunar elevation and phase, frequent auroral activity at the polar latitudes, airglow emissions and other background sources.

Beyond 3 microns, where scattering falls off rapidly with wavelength, thermal emission by the atmosphere becomes dominant. A 300°K blackbody distribution (ambient temperature of earth) at sea level and a 213°K blackbody at 30 km altitude are approximations to this condition within the 3 to 2000 micron interval. This radiation is present during the day or night and the diurnal variation is that expected from the changing temperature, and the differing optical depths in window and absorption regions.

Low altitude clouds (less than 20 km) illuminated by the sun reflect strongly in the visible and near infrared wavelengths as viewed from satellite altitudes and emit blackbody radiation at the longer wavelengths. Direct sunlight falling on a cloud of 80% reflectivity may produce radiances of 10^{-2} watts/cm^2-micron-steradian, or higher for extremely thick clouds or those with specular-like reflectivity properties due to the illumination geometry or cloud structure.

Satellite systems, under certain circumstances, may not only detect desired stellar radiation but also line and band emissions that originate at airglow layer altitudes. Visible airglow radiation may emit at intensity levels undesirable in terms of stellar signal to background ratios associated with an optical detection system. The majority of airglow emissions are in the vicinity of 100 km; thus systems operating at satellite altitudes and looking at a stellar background below a line-of-sight tangent to the uppermost layers will incur airglow within the field of view. Therefore, detection in the direction of large nadir angles and where the line-of-sight is above the absorbing the scattering atmosphere incurs radiance principally attributed to day, twilight and night airglow.

Optical interference effects due to noctilucent clouds may also occur when attempting to operate against stellar backgrounds in the general vicinity of the earth and especially when passing over high northern latitude regions during the summer months. Noctilucent cloud formations occurring near 80 km may scatter solar radiation in the visible with spectral radiance as high as 10^{-5} watts/cm^2 - micron-steradian at 0.5μ. Based on noctilucent cloud observations it is evident that the cloud parameters vary considerably with latitude, time of day season and to a lesser extent with altitude.

Auroral intensity sometimes fluctuates over wide limits or remains steady in the form of a diffuse glow. Spectral fluctuation or the possibility of a dynamic spectral redistribution present potential

difficulties in the stellar detection process. In general, aurora radiates in the 100 km altitude region and may emit at an average intensity level of 3.5×10^{-8} watts/cm^2-ster in the spectral range 0.3 to 0.5 microns. The greatest frequency of aurora occurs in two auroral zones, a region 20 to 25 degrees approximately concentric about the geomagnetic poles which in the Northern Hemisphere is in Northern Greenland. The frequency of occurrence decreases sharply to the north and south on either side of the zone concerned, falling to about 20% of its peak value in a latitude change of 10°.

Many of the natural backgrounds described above may be neglected in determining the extent of background interference during stellar viewing. That is, the satellite navigation system geometry limits observation angles to lines-of-sight above the earth's surface, eliminating backgrounds attributed to thermal emission and albedo of the earth. In order to reduce distortions in the stellar signal created by atmospheric refraction and scintillation and to avoid cloud reflection, look angles may be further restricted to directions above these disturbing atmospheric regions. Selection of the spectral wavelength region 0.3 to 0.5 microns eliminates many infrared and ultraviolet radiations attributed to atmospheric thermal emission, airglow, ozone albedo and major portion of the scattering atmosphere.

The following sections described only those background radiations which may interfere with stellar detection and concludes with a comparative study of optical signal levels received by a satellite

navigation and point out the difficulties encountered during certain satellite-stellar background geometries.

SECTION 2

NATURAL BACKGROUND

2.1 AIRGLOW SPECTRAL FEATURES

Satellite systems will not only detect those radiations observable from the ground, but also numerous other emission lines and bands that originate at airglow layer altitudes and are normally masked by absorption further down in the earth's atmosphere. Even though the airglow layers emit at low levels of intensity when compared with such natural atmospheric backgrounds as those attributed to thermal emission and solar scattering, many of the airglow features may still form principal background radiance for certain stellar look angles in the direction of large nadir angles. Of importance is the determination of any airglow radiation in the 0.3 to 0.5μ spectral region that may emit at intensity levels undesirable in terms of stellar signal-to-background ratios associated with a detection system. Although nadir airglow radiance will not be observed by stellar navigation systems, a description of all important airglow spectral features in the direction of nadir is deemed necessary as a reference since these same emissions but with increased intensity will be encountered for the satellite-stellar background geometries discussed in this report.

Herzberg bands occurring in the spectral wavelength region 3000 to 4700 A are so close together that they have the appearance of a continuum with an average spectral radiance of about 4.0×10^{-11} watts/cm^2- steradian for the nocturnal value.

N_2^+ ions may be produced by particle bombardment. If there is such a production, an intensity of about 4.0×10^{-14} watts/cm^2- ster may be expected from the First Negative band system, most of which will appear at 3914 A. Fishkova and Markova (1960) have performed sea-level observations of the N_2^+ 0 - 0 transition at 3914 A in the nocturnal airglow spectrum.

Danilov (1961) attributes the occurrence of the NI lines to dissociative recombination of N_2^+ ions. These lines, aside from the 5200A line, include the 3466 A line with an intensity predicted at 9.2×10^{-11} watts/cm^2- steradian during the nighttime.

In addition to the line and band airglow spectrum of the nightglow, a continuum exists (due to O and NO reactions) extending from just below 0.4μ to about 0.7μ. This green continuum has been observed (Packer, 1961) with the emitting layers occurring at altitudes between 70 and 150 km. Dayglow radiance may exceed nightglow (Chamberlain, 1961) by a factor of 20.

Table 2-1 is a summary of all known nocturnal airglow emissions in the spectral wavelength region 0.3 to 0.5μ detectable by satellite systems. The table also gives some details regarding the spectral states

TABLE 2-1

NIGHTGLOW, TWILIGHT AND DAYGLOW SPECTRAL FEATURES, 0.3 TO 0.5 MICRONS

Designation	Atomic or Molecular Transition	Spectral Region (A)	Nightglow Average Radiance, N (watts/cm^2 -ster)	Twilightglow Average Radiance, N (watts/cm^2 -ster)	Dayglow Average Radiance, N (watts/cm^2 - ster)
O_2 Herzberg Bands	$A^3\Sigma_u^+ \rightarrow X^3\Sigma_g^-$	3000-4700	4.3×10^{-11}	4.3×10^{-11}	4.3×10^{-11}
O_2 Bands	$B^3\Delta_u \rightarrow a^1\Delta_g$	4000-5000	3.5×10^{-12}	3.5×10^{-12}	3.5×10^{-12}
Continuum		4000-7000	1.0×10^{-10}	2.0×10^{-9}	2.0×10^{-9}
		4000-5000	1.2×10^{-11}	2.4×10^{-10}	2.4×10^{-10}
N_2^+ First Negative Band	$B^2\Sigma_u^+ \rightarrow X^2\Sigma_g^+$	3914 (0-0)	4.0×10^{-14}	4.1×10^{-11}	5.1×10^{-9}
		4278 (0-1)		1.0×10^{-11}	1.0×10^{-9}
NI Line	$^2D_{3/2} \rightarrow {}^4S^o_{3/2}$	3466	9.2×10^{-13}	9.2×10^{-13}	9.2×10^{-13}
CaII	$^2P^o_{\frac{1}{2},\ 3/2} \rightarrow {}^2S_{\frac{1}{2}}$	3968.5		6.0×10^{-12}	
		3933.7			

of the various atoms and molecules along with the average radiation emitted by the various layers. Most of the emissions are variable and only order of magnitude can be given for the average intensities at the airglow layers.

In general, the majority of nocturnal airglow emissions also occur during the twilight period. Even though some twilight emissions show enhancement, others remain relatively unchanged in intensity. Identification of twilight features accompanied by average radiance values are given in Table 2-1. The calcium resonance line, not observed in the nightglow, is also shown in Table 2-1.

Except for the observation (Blamont and Donahue, 1961) of the dayglow Sodium D lines, numerous dayglow predicted features have not yet been successfully observed via rocket and balloon attempts (Wallace, 1961) and cannot be observed from the ground against the intense sky background. Dayglow is expected to present a spectral background similar to that of the twilight and nightglow spectrum. Dayglow features are also given in Table 2-1 together with predicted dayglow intensities.

2.2 LONG SLANT PATH AIRGLOW RADIANCE

Major variations in radiance, spectral or spatial background parameters can possess directional characteristics depending on the altitude, look angle, and spectral region intrinsic in a space-based stellar detection system. Since airglow emission originates from uniform emitting layers which surround the earth in the neighborhood of 100 km altitude,

an orbiting satellite looking straight down (nadir angle = 0^{o}) will see minimum airglow radiation per unit solid angle. However, a detector system with a small field of view at large nadir angles receives irradiance from much larger optical paths, such that it is possible for the detector to view an airglow layer along an 800 km path length within the layer. The result is an increase in intensity of bands and/or lines (depending on the operational spectral region) by as much as a factor of 40 over the radiance from the nadir direction.

The extent of actual interference by the airglow background on stellar detection depends solely on stellar background radiance levels simultaneously encountered and the spatial distribution of all radiance. In particular, the critical parameters involved are the stellar background-satellite geometry and the spectral region in which the high altitude satellite-borne detector may be performing. For instance, at the longest airglow slant paths the primary quiescent background encountered, day or night, is attributed to airglow for the spectral region 0.3 to 0.5μ wherein scattered solar radiation diminishes since the line-of-sight is above most of the scattering atmosphere. The multitude of possible effects on a stellar navigation system detecting a stellar field against a composite of natural day-night backgrounds is discussed in the final section of this report (Section 3).

An average order of magnitude airglow radiance is estimated in this section for the 0.3 to 0.5μ spectral region as seen by a satellite

looking below a line-of-sight tangent to the top of emitting layers. It is therefore desirable to compute the effect of long slant paths on a given radiance distribution and to ultimately plot the airglow radiance as a function of look angle (nadir angle) for a range of vehicle altitudes. (The long slant path results formulated in this section and supplemented by the spectral radiance values given in Section 2.1 accomplishes this goal.)

The theoretical calculation of airglow background radiance, N (watts/cm^2-ster) involves the summation of the volume radiance contribution from each of the infinitesimal emitting volume elements located along the line-of-sight provided the field of view is infinitesimal emitting volume elements located along the line-of-sight and provided the field of view is infinitesimal (see Figure 2-1A),

$$N = N_{nadir} \int_0^{\ell} N'_v d\ell \int_0^{t} N'_v dt \qquad (2\text{-}1)$$

where N_{nadir} = nadir radiance emitted at the airglow layer in watts/cm^2-ster

N'_v = normalized volume radiance (emission rate) in watts/cm^2-ster-km

$d\ell$ = elemental emitter along line-of-sight

ℓ = depth in km of effective emitting airglow layer, i.e., long slant path length

t = effective layer thickness

Figure 2-2 shows the satellite-airglow geometry and represents a typical normalized altitude-volume radiance profile averaged from several rocket

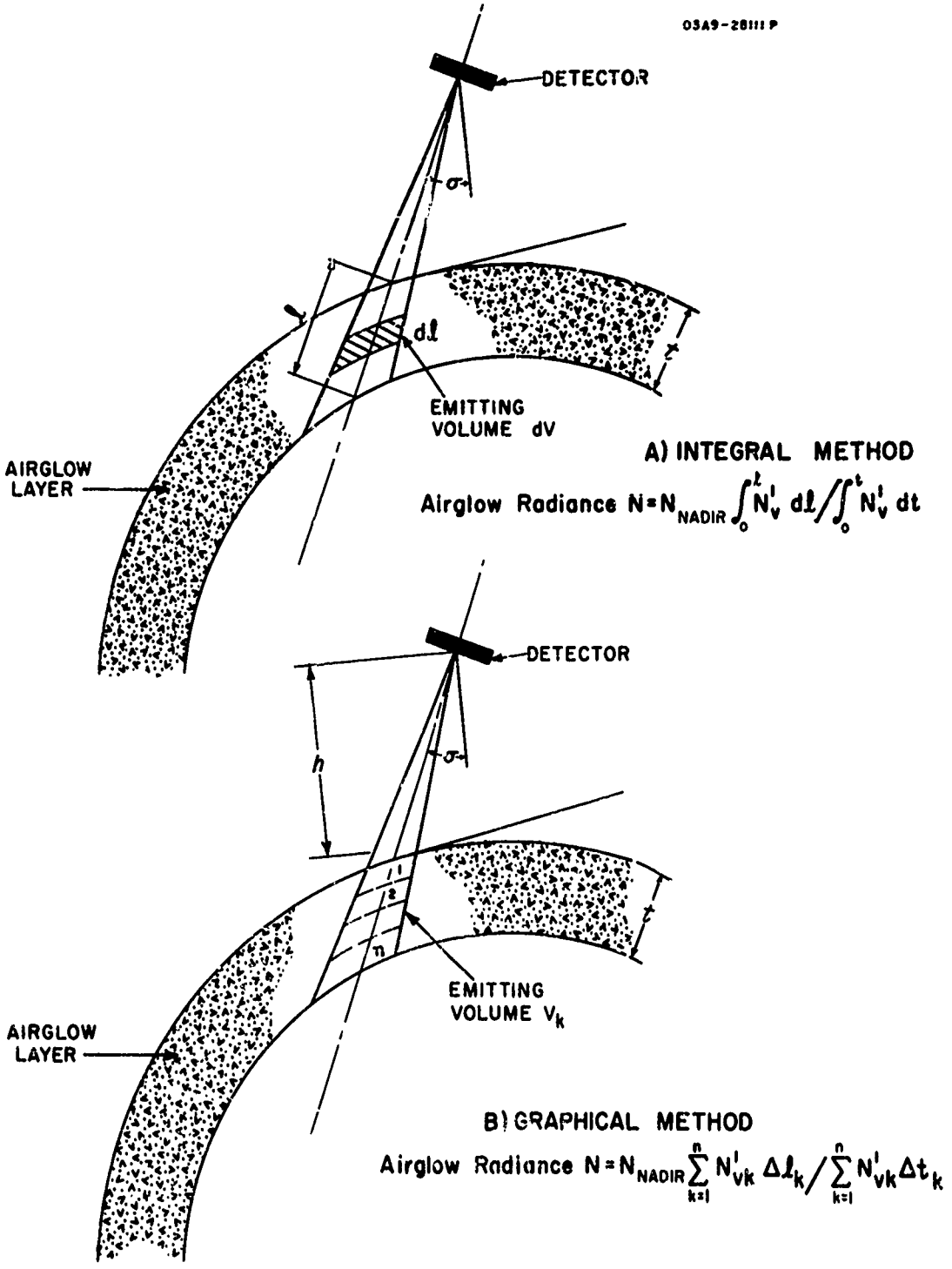

Figure 2-1. Satellite-Airglow geometry.

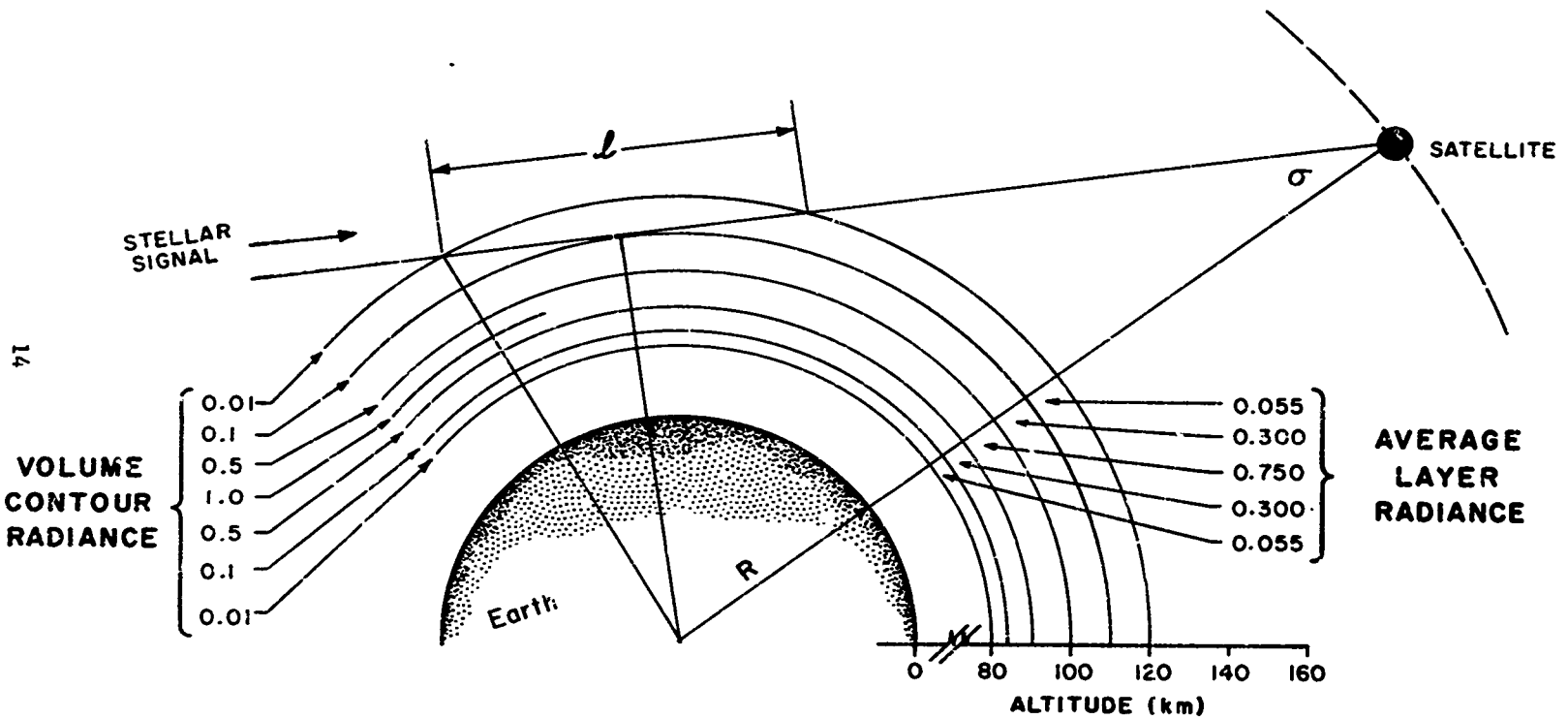

03A19-410P

Figure 2-2. Satellite-Airglow geometry showing volume isoradiance contours representing airglow emission dependence on altitude.

profiles (Packer, 1961) and segmented into volume isoradiance contours in order to determine the average path length through the curved emitting airglow layer. Seasonal and latitudinal variance in the altitude profile shape has little influence on the background radiance as seen from high altitudes, especially in view of the detector's altitude, relative to layer depth and position. The selected average profile is adequate for the determination of average radiance as a function of long slant paths.

Since the functional dependence of emission on altitude is not exactly formulated for long slant paths through a curved layer, the exact formal integration becomes difficult. Utilization of the airglow volume isoradiance chart, however, eliminates the necessity for formal integration by substitution of a simple summation over a finite number of average emitting volumes along the path length (see Figure 2-1B), an approximation sufficiently accurate for our purposes wherein we assume average volume radiance for each uniform airglow elemental layer. The required path lengths are easily calculated with trigonometric identities utilizing known values for the airglow layer and satellite altitude, and the earth's radius. Multiplying each increment of distance along the line-of-sight measured between two contour lines by the average radiance values of each sub-layer and summing over the entire path length gives a total airglow radiance effect. This long slant path effect on radiance in terms of nadir radiance, N_{nadir}(watts/cm^2-ster) is given in Table 2-2 and is given for several satellite look angles and the altitudes 200, 600, 3100 and 5000 km. It is only necessary to substitute the

TABLE 2-2

LONG SLANT PATH EFFECT ON AIRGLOW RADIANCE

Observation Angle, σ				Average Layer Volume-Radiance, N'_v (watts/cm^2 - ster-km)	Path Length, $\Delta\ell$ (km)	Normalized Radiance, $\Sigma N'_v \Delta\ell$ (watts cm^2-ster)		Long Slant Path Radiance	Nightglow Radiance, N (watts/cm^2-ster) 0.30 to 0.50μ	Dayglow Radiance, N (watts/cm^2-ster) 0.30 t 0.50μ
200 km	600 km	3100 km	5000 km							
0	0	0	0	0.055 0.300 0.750	14 16 10	0.77 4.80 7.5	13.1	N_{nadir}	6.0×10^{-11}	6.4×10^{-9}
76°34'	66°39'	42°28'	34°13'	0.055 0.300 0.750	176 208 132	9.68 62.4 99.0	171.1	13.1 N_{nadir}	7.9×10^{-10}	8.4×10^{-8}
79°30'	67°58'	43°2'	34°38'	0.055 0.300 0 750	230 300 718	12.65 90.0 538.5	641.2	49 N_{nadir}	2.9×10^{-9}	3.1×10^{-7}

desired absolute nadir radiance (Table 2-1) which for the 0.3 to 0.5μ region is 6.0×10^{-11} watts/cm^2-ster (nightglow) and 6.4×10^{-9} watts/cm^2 -ster (dayglow).

2.3 NOCTILUCENT CLOUD RADIANCE

Noctilucent cloud phenomenon is generally attributed to the scattering of solar radiation from a layer of particles located at 85 km, thus forming a natural background which may interfere with stellar detection. For instance Ludham (1957) and others (Mirtov, 1962; Hoffmeister, 1961) have discussed the accumulation of micrometeorite dust at 85 km forming dusty layers which may be responsible for sea level observations of noctilucent cloud phenomena. Rocket measurements (Milinov, 1962) in the altitude region 80 to 100 km have confirmed the existence of an aerosol layer over the middle and northern latitudes of Russia.

Measurements on noctilucent clouds made from the ground have yielded dust layer parameters of value to the analysis performed in this section. Deirmendjian and Vestine (1959) upon analyzing noctilucent cloud spectra recorded by Grishin (1956) deduced that the effective particle size may be as great as 0.4 microns and that an index of refraction of 1.33 explains the observed reflecting properties of the layer Witt (1960) measuring the polarization of light from noctilucent clouds in two visible spectral regions deduced a particle radius in the vicinity of 10^{-5}cm provided an index of refraction of 1.33 is assumed. The upper limit of the particle size turns out to be 1.8×10^{-5} cm representing stony particles corresponding to an index of refraction of 1.55. According to

Ludham (1957) high altitude dust layers consist of particles 10^{-6} to 10^{-5} cm and calculates particle densities to be 1 cm^{-3} and 10^{-2} cm^{-3} respectively. Effective layer thickness (Mikirov, 1962) ranges from 3 to 10 km depending on latitude, concentration, season, etc. with the peak dust concentration located at altitudes (Hessvedt, 1961; Mikirov, 1962) ranging from 80 to 90 km.

Noctilucent clouds seem to occur only at high northern latitudes during the summer months and only at twilight. Clouds are seen from the ground under restricted viewing conditions so that it is difficult to imply the true spatial extent of some clouds unless they are small. That is to say, an existing cloud at 82 km in direct sunlight which is dense enough to scatter solar radiation appreciably, may go undetected at sea-level provided the brightness of the background due to atmospheric scattering is many orders of magnitude greater than the cloud radiance. Also, those twilight solar rays passing through the earth's absorbing atmospheres are not intense enough to scatter the amount of energy required for detection at sea-level. Furthermore, adverse weather or atmospheric haze often prevents the observation of noctilucent clouds.

Satellite detection systems may encounter reflecting clouds during twilight and day periods under certain viewing conditions. Certainly a vehicle in direct sunlight and looking at long slant paths may encounter reflected light from clouds, since backscattering of light into the satellite's line-of-sight can occur. Furthermore, a satellite located on the dark side of the earth may also view at long slant paths

noctilucent cloud phenomena occurring over the twilight zone. For those geometries where the look angle increases such that smaller and smaller scattering angles are encountered, forward scattering of sunlight becomes appreciable. At the same time longer slant paths are incurred which means larger quantities of scattering particles are along the optical line-of-sight, greatly increasing the optical thickness.

Maximum cloud radiance expected as a function of satellite altitude and look angle may be determined by performing an angular Mie scattering analysis on a cloud model which is based on the sea-level observational data discussed above. The expected spectral radiance from a 5 km thick cloud was calculated for various scattering angles and is shown in Figure 2-3 illustrating the importance of the scattering angles. Soviet measurements recorded at sea-level and reported by Sharonov (1960) are in good agreement with these results for the visible region.

Of particular value is the noctilucent cloud radiance as a function of satellite-stellar background geometry, i.e., as a function of satellite altitude and look angle. Reference to the scattering angles (Figure 2-3) associated with the desired look angle values gives noctilucent cloud radiance for the spectral region 0.3 to 0.5μ as a function of the look angle for several satellite altitudes. Thus a satellite may encounter noctilucent cloud radiance as high as 4.0×10^{-7} watts/cm^2 -ster for the observation angles and altitudes associated with stellar detection in the 0.3 to 0.5 micron region.

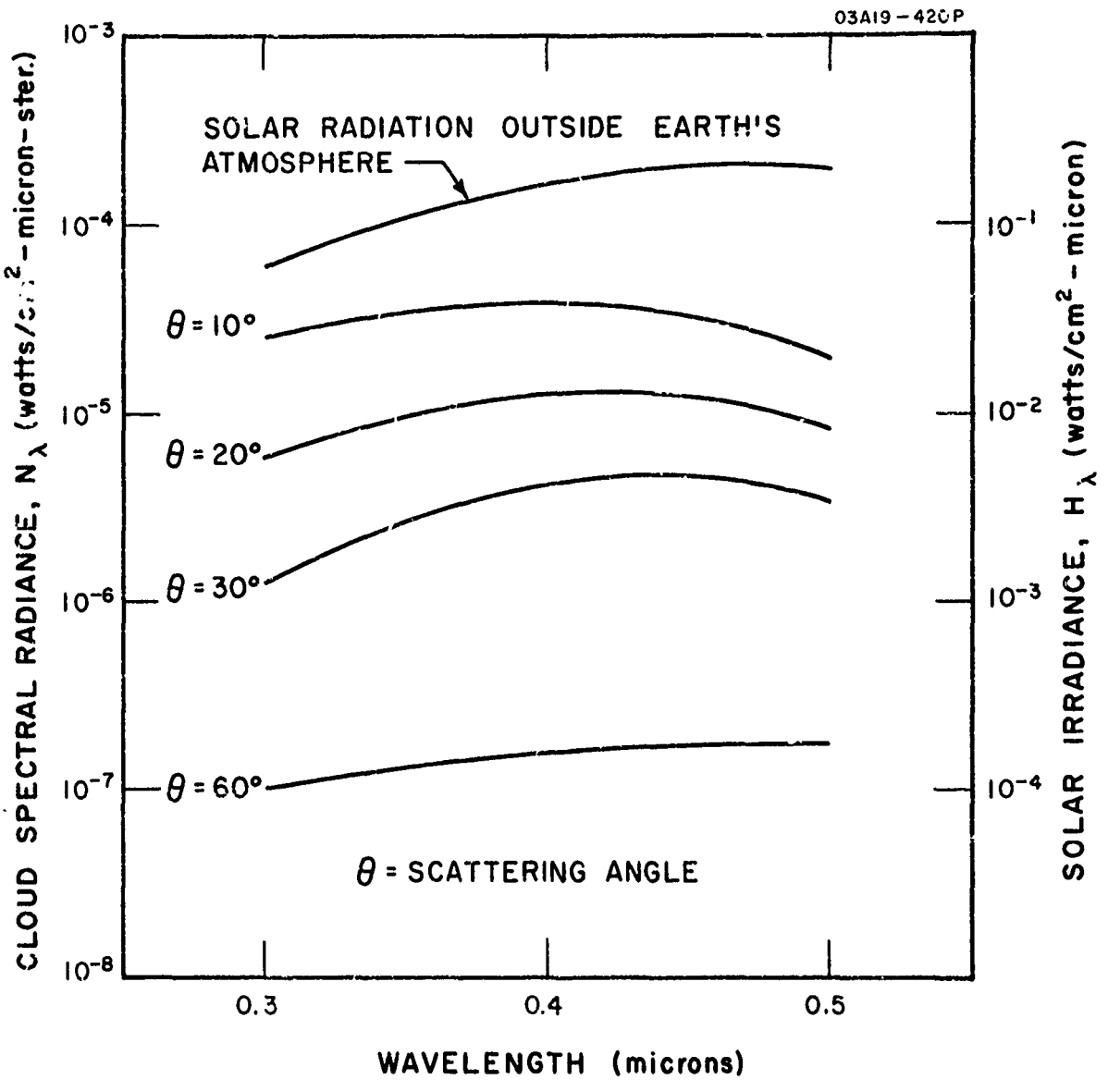

Figure 2-3. Spectral radiance due to solar scattering by dust layers at 85 km. Importence of scattering angle is evident.

2.4 AURORA

The irradiance at the satellite aperture due to auroraeinvolves the assumption that the emitting aurora area imaged by a single cell is much greater than the associated field of view (10^{-5} ster). Typical auroral displays of a discrete nature (homogeneous arcs and bands) occur most often at high latitudes and many possess frontal areas of $\sim 10^4$ km^2. Slant path considerations are not effective in the case of aurorae of this type insofar as the latitudinal surface thickness may be only a few kms. For aurorae located at high altitudes (cases observed between 600 - 1000 km) the satellite may view auroraeat practically all geographical latitudes of appearance because of symmetry considerations for aurorae in both the Nothern and Southern hemispheres. The frequency of appearance for the high altitude red diffuse auroraeat low latitudes, however, is low. In general, auroraeradiate in the 100 km altitude region and may emit as an upper limit an average intensity level of 3.5×10^{-8} watts/cm^2-ster in the spectral range 0.3 to 0.5 microns.

2.5 RAYLEIGH SCATTERING

A brief discussion of Rayleigh scattering in the earth's atmosphere, as applied to satellite navigation, is given in another report of this series (Naqvi 1962 II, hereafter referred to as Report II). For the wavelength region 0.3μ to 0.5μ, absorption is negligible. The calculations of the radiation flux emerging from the top of the earth's atmosphere as a result of Rayleigh scattering of the light from the sun or

the moon is very complicated. The problem has been treated in detail for a plane parallel atmosphere by Chandrasekhar (1950), Chandrasekhar and Elbert (1954), and numerical calculations have been performed by Coulson (1959) and by Coulson, Dave and Sekera (1960).

To understand the nature of the problem consider Figure 2-4 which is drawn for a spherical atmosphere.

A coordinate system xyz is attached to an instantaneous position of the satellite as shown. The horizontal plane xy is perpendicular to the satellite-earth direction. Let the direction of the incident light be such that its zenith angle is σ_o and its azimuth is zero. Let us consider the scattered radiation received from a direction $(\pi - \sigma, \varphi)$, through a solid angle $d\omega$. The total intensity of radiation is made up of contributions from the volume elements such as dV. The problem is complicated due to the following factors

(1) The radiation flux incident at any volume element dV is less than or equals that incident at the "top" of the earth's atmosphere, on account of Rayleigh scattering in the overlying region. The actual incident flux depends upon the optical thickness of the atmosphere at dV, along the path of radiation. This is different at different locations and depends strongly upon wavelength on account of λ^{-4} dependence of scattering cross-sections.

(2) The radiation scattered by volume element dV, in a solid angle $d\omega$, in the direction of the satellite is further attenuated (again on account of Rayleigh scattering) on its way to the satellite detection system.

(3) The multiple scattering of radiation has to be considered.

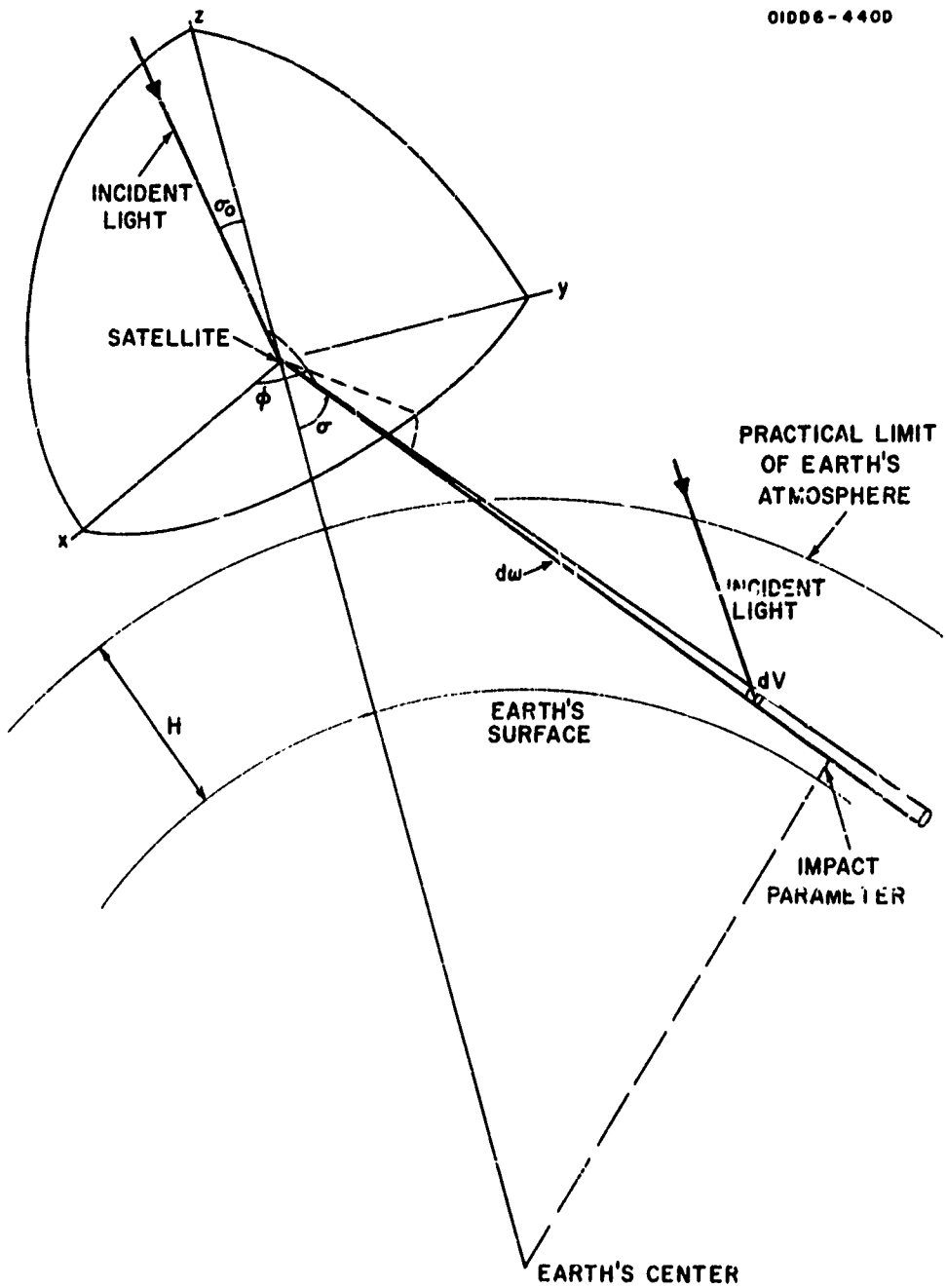

Figure 2-4. The scattering geometry.

Table 2-3 based upon Diermendjian's (1955) calculations shows the wave length dependence of the normal optical thickness τ (for Rayleigh scattering only) at sea level

TABLE 2-3

τ	1.00	0.50	0.25	0.15	0.05
λ (μ)	0.3125	0.3715	0.4365	0.4950	0.6440

Thus the normal optical thickness in the wavelength region 0.3μ to 0.5μ is approximately between 0.15 and 1.

The observation angles σ for various satellite heights h and impact parameters of the scattered light beam with respect to the earth, h_o = 0, 20 and 120 km, are given in Table 2-4.

In Figures 2-5 and 2-6, both taken from the work of Coulson (1959) for a plane parallel atmosphere, the relative intensity is plotted for various relevant variables (the normal optical thickness τ of the atmosphere, the zenith angle σ_o of the light source, the nadir angle σ of the direction of observation along which the scattered light is received, and the azimuth angle φ of the direction of observation). In both figures the reflectivity of the earth's surface is neglected, which if taken into account would increase the relative intensity shown.

Figure 2-5 is drawn for φ =0 and π and Figure 2-6 for φ = 0 only. For other azimuth angles the relative intensity is slightly different, but fo simplicity we shall ignore all variations with azimuth angles.

TABLE 2-4

THE OBSERVATION ANGLES FOR VARIOUS SATELLITE HEIGHTS AND IMPACT PARAMETERS OF THE LIGHT BEAM

Satellite Height h(km)	Impact Parameter h_o(km)	Observation Angle σ	$\mu = \cos \sigma$
200	0	75° 50'	0.245
	20	76° 34'	0.232
	120	81° 3'	0.156
600	0	66° 4'	0.406
	20	66° 29'	0.399
	120	68° 37'	0.365
3100	0	42° 17'	0.740
	20	42° 28'	0.738
	120	43° 17'	0.728
5000	0	34° 6'	0.827
	20	34° 13'	0.827
	120	34° 20'	0.821

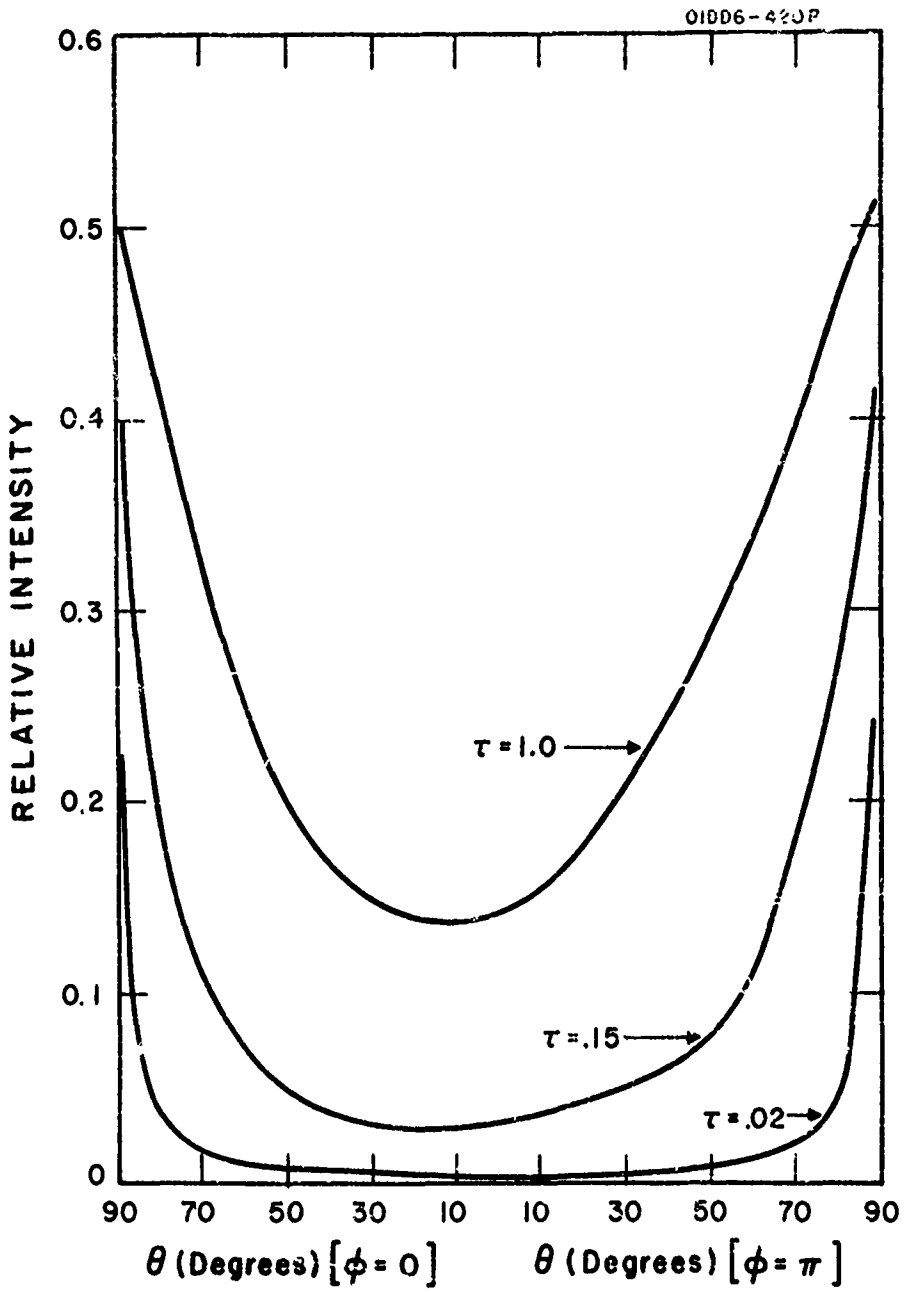

Figure 2-5. Relative intensity for different optical thicknesses as a function of direction in the sun's vertical. ($\cos \sigma_o = 0.40$)

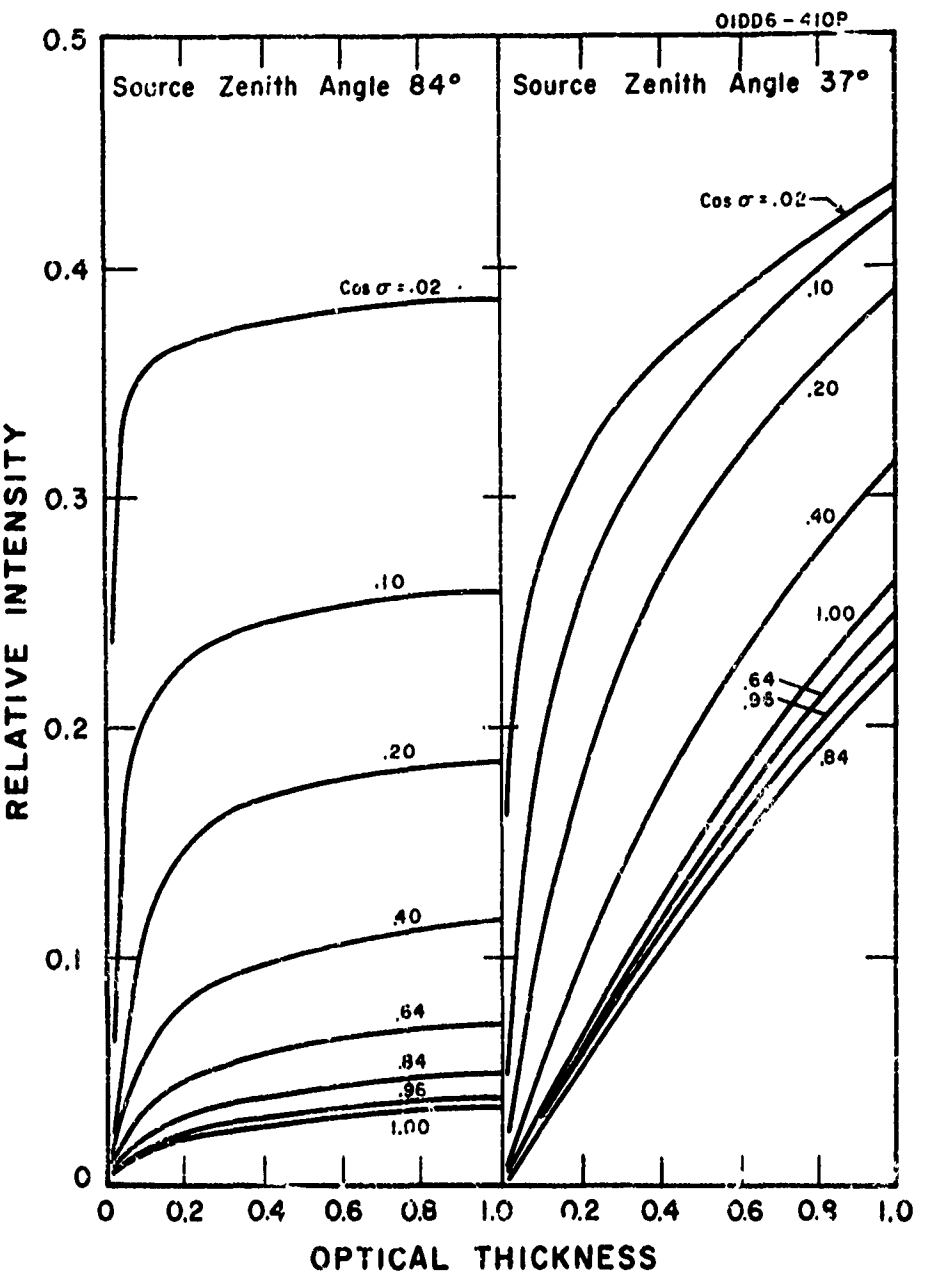

Figure 2 6. Relative intensity as a function of optical thickness for two values of source zenith angle and eight different directions in the sun's vertical (φ . 0).

Another point worth noting is that the large increase of relative intensity for σ approaching 90° is the result of the assumption of a plane parallel atmosphere. The theory is not applicable to a spherically stratified atmosphere for large values of σ.

To convert from relative to absolute intensity or radiance (in watts/cm^2 ster wavelength interval), the former must be multiplied by F where πF is the incident flux (in watts/cm^2 wavelength interval) at the "top" of the earth's atmosphere.

The relative intensities of scattered radiation are given in Table 2-5 for four satellite heights (200, 600, 3100 and 5000 kms), two look directions (corresponding to the impact parameters of the light rays = 0 and 120 km respectively), two wavelengths 0.3μ and 0.5μ (corresponding to normal optical thickness = 1.0 and 0.15 respectively), and two zenith angles of the source 84° and 37°. Note that more accurate values could have been obtained by interpolating among the tables of Coulson, Dave and Sekera (1960), but since the variation of relative intensity with azimuth angle is neglected, there is little justification in carrying on such a calculation.

The relative intensity varies with τ and therefore with wavelength. The correct procedure for calculating the radiance in the wavelength interval 0.3μ to 0.5μ is therefore to use the appropriate incident flux, which also varies with wavelength, and integrate (or sum) over the wavelength interval. For the sake of simplicity we shall, however, take an average value of relative intensity, with shorter wavelengths carrying

TABLE 2-5

RELATIVE INTENSITIES OF SCATTERED LIGHT

Satellite Height h(km)	Look Direction $\mu = \cos\theta$	$\lambda(\mu)$	τ	Relative Intensities $\theta_o=84^\circ$	$\theta_o=37^\circ$
200	0.24-0.16	0.3	1.0	0.17-0.23	0.37-0.4
		0.5	0.15	0.12-0.17	0.13-0.17
600	0.41-0.36	0.3	1.0	0.11-0.14	0.32-0.37
		0.5	0.15	0.06-0.09	0.05-0.08
3100	0.74-73	0.3	1.0	0.06	0.26
		0.5	0.15	0.033	0.033
5000	0.83-0.82	0.3	1.0	0.05	0.23
		0.5	0.15	0.025	0.025

a greater weight, and for a satellite altitude of 200 km we shall assume this to be 0.3. Similarly we shall use the total incident flux in the wavelength interval mentioned above which for the sun turns out to be,

$$\pi F(\text{sun}) = 3.1 \times 10^{-2} \text{ watts/cm}^2$$

The incident flux from the moon, being reflected sunlight, has essentially the same spectral characteristics as the sunlight, at least in the wavelength region of interest to us. The brightness of the full moon is, however, less by a factor of 2×10^{-6}* and the incident flux from the full moon is

$$\pi F(\text{full moon}) = 6.2 \times 10^{-8} \text{ watts/cm}^2$$

The radiance of the earth's atmosphere due to scattered light is

$$N(\text{sun}) = 3 \times 10^{-3} \text{ watts/cm}^2 \text{ ster}$$

$$N(\text{full moon}) = 6 \times 10^{-9} \text{ watts/cm}^2 \text{ ster}$$

It should be mentioned that the flux of radiation from the moon diminishes rapidly with changing phases on either side of the full moon. At quarter phase the flux is only about 11% of the full moon value. This is shown in F 7 where % radiation flux is plotted against the angle from the sun.

---

* The visual magnitude of the sun and the moon are -26.9 and -12.7 respectively (Allen, 1957).

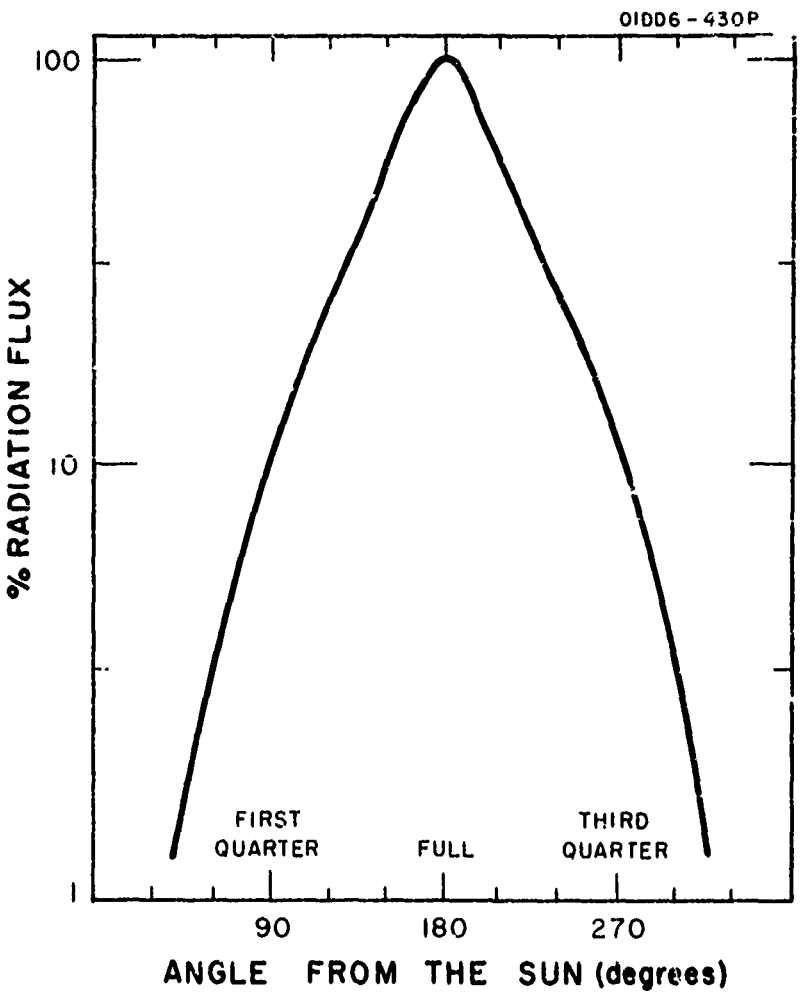

Figure 2-7. Percentage radiation flux from the moon at various phases.

SECTION 3

COMPARISON OF STELLAR AND ATMOSPHERIC RADIATION

In this section we will compare the irradiance of the typical bright stars likely to be used in satellite navigation by the terrestrial occultation method with the irradiance of the atmosphere due to the various sources discussed earlier. A discussion of the instrumental techniques is beyond the scope of this report. For our purpose it is sufficient to consider a telescope and a suitable photoelectric photometric system. We shall assume a field of view of 10 μ steradians.

Figure 3-1 illustrates typical occultation geometry. In position (1), stellar signal is practically unattenuated and the irradiance of the atmosphere due to all sources is practically zero, in the wavelength region 0.3μ to 0.5μ. In position (2), the signal is still practically unattenuated but the detector receives radiation from the atmospheric sources (principally the (long slant path) airglow, the noctilucent clouds depending upon the relative position of the sun, and the aurorae if present). In position (3), the star light is attenuated by Rayleigh scattering (Report II) and some radiation is received from atmospheric sources also (principally due to Rayleigh scattering of sunlight and moonlight depending upon the relative positions of the two bodies with respect to the earth as well as with respect to each other, since this

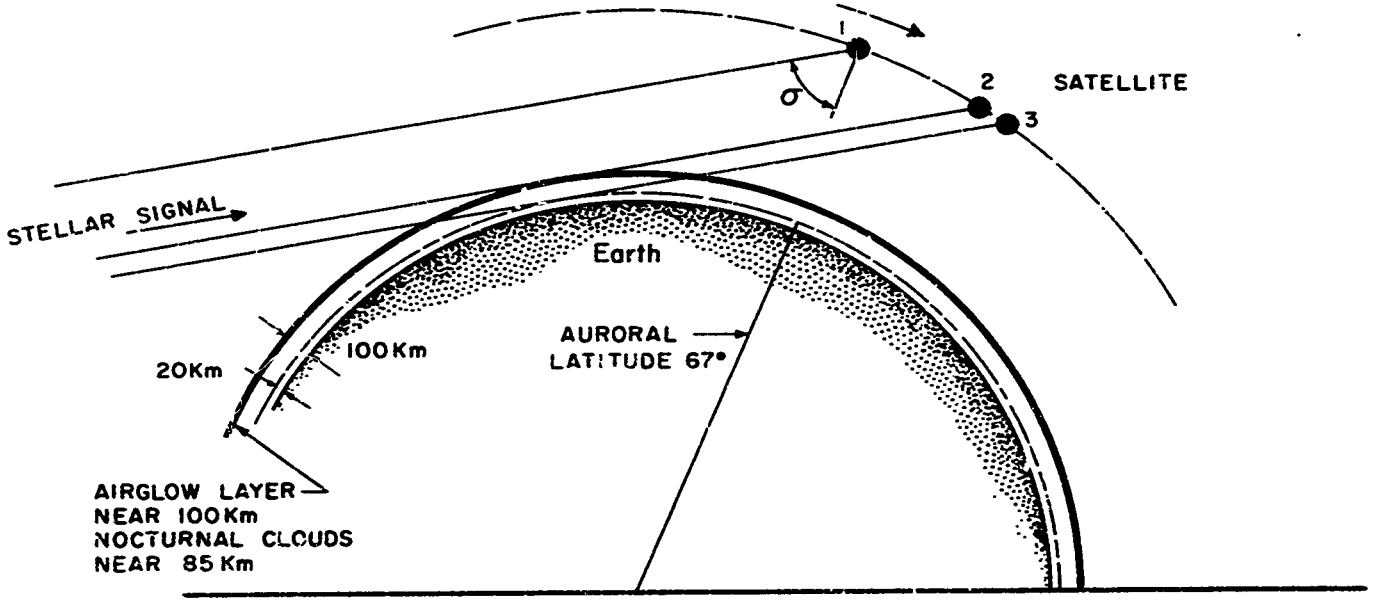

Figure 3-1. Typical occultation geometry.

latter governs the lunar phases, and also due to airglow and aurorae).

The estimates of atmospheric radiance in the 0.3 to 0.5μ region are summarized in Table 3-1. The stellar signal to atmospheric noise ratio (S/N) for Sirius (m_v = -1.43; m_{pg} = -1.55; color: blue; visually the brightest star) and Betelgeuse (m_v = 0.7; m_{pg} = 2.44; color: red; visually the brightest star of spectral class M) and for various atmospheric sources are given. The instrumental field of view is assumed to be 10 μ steradians. For any other field of view, the entries of Table 3-1 should be multiplied by one-tenth the field of view expressed in μ steradians. Column 5 of Table 3-1 gives the photographic limiting magnitude corresponding to stellar signal to atmospheric noise ratio of unity. The last column gives the corrected value of the limiting magnitude for the case where the starlight is attenuated by 0.8 magnitudes on account of extinction in the atmosphere (Report II).

The radiance due to Rayleigh scattering of the sunlight is so large as to mask completely the starlight. It seems certain that no useful observations of star occultations can be performed against the foreground of the sunlit atmosphere including the twilight region. (For the same reason the earth-bound astronomer waits until nighttime to make his observations). If observations are confined to the night side of the earth, the interference on account of day airglow and noctilucent clouds need not be considered.

Auroral radiance is significant but variable. From time to time it will interfere with occultation observations. For this reason we

TABLE 3-1

ATMOSPHERIC RADIANCE IN THE 0.3 TO 0.5μ REGION

(COMPARISONS WITH TWO BRIGHT STARS)

Source	Radiance N (watts/cm^2 ster)	Stellar Signal to Atmospheric Noise Ratio S/N (field-of-view = 10^{-5} ster) Sirius*	Betelguese*	m_{pg} for S/N = 1 Uncorrected For Atmospheric	Corrected Exinction
Airglow (night)	2.9×10^{-9}	150	3.8	3.9	3.1
(day)	3.1×10^{-7}	1.4	0.036	-1.2	-2.0
Noctilucent Cloud	4.0×10^{-7}	1.1	0.028	-1.4	-2.2
Aurora	3.5×10^{-8}	13	0.31	1.2	0.4
Rayleigh Scattering					
(Sun)	3×10^{-3}	1.5×10^{-4}	3.7×10^{-6}		
(Full Moon)	6×10^{-9}	73	1.8	3.1	2.3

Stellar Irradiance

Sirius = 4.4×10^{-12} watts cm^2

Betelgeuse = 1.1×10^{-13} watts/cm^2

should have more stars available than the minimum number required.

Night airglow is a constant feature of the night sky and forms the principal quiescent background viewed by high altitude satellites. The corrected stellar photographic magnitude for which the signal to noise ratio is unity is 3.1. There are about 320 stars brighter than this magnitude over the entire sky. They are, however, not uniformly distributed over the sky but show a tendency for clustering around the galactic plane (See Naqvi, 1962 I, hereafter referred to as Report I).

Astronaut Glenn (1962) first reported seeing, from the night side of the earth, a bright layer 6 to 8 degrees above the horizon and $1\frac{1}{2}$ to 2 degrees wide. He noticed that as the stars come down close to the horizon, they became relatively dim for a few seconds, then brightened up again before they were occulted by the earth. These reports have been confirmed by Astronaut Carpenter (O'Keefe, 1962) who established that this is the airglow layer. He carried a filter for the λ5577 auroral line, and noted that whereas the light of the moonlit earth could not pass through the filter, light of the luminous band passed through it with little attenuation. Based on Carpenter's observation the surface brightness of the nightglow layer is estimated at x 10^{-3} lux per steradian. This is equivalent to 9 x 10^{-10} watts per cm^2 per steradian, and, in view of the uncertainties of measurements and of our calculations, agrees rather well with the value given in Table 3-1.

The radiance of the scattered moonlight varies with the lunar phases. At full moon the corrected stellar photographic magnitude for which the signal to noise ratio is unity is 2.3. There are approximately 60 stars brighter than this magnitude, although again not uniformly distributed over the sky. Scattered moonlight, and to some extent the night airglow are likely to cause sufficient interference with occultation observations. Since the calculations presented in this report are preliminary in character, we feel that more refined calculations are warranted, as well as more precise observations from the satellites.

REFERENCES

Allen, C. W. (1957), Astrophysical Quantities, Athlone Press, London.

Blamont, J. E. and Donahue, T. M. (1961), "The Dayglow of the Sodium D Lines", J. Geophys. Res. 66, 1407.

Chamberlain, J. W. (1961), Physics of the Aurora and Airglow, Academic Press, New York.

Chandrasekhar, S. (1950), Radiative Transfer, Clarendon Press, Oxford.

Chandrasekhar, S. and Elbert, D. (1954), "The Illumination and Polarization of the Sunlit Sky on Rayleigh Scattering", Trans. Amer. Phil. Soc., New Series 44, 643.

Coulson, K. L. (1959), "The Flux of Radiation from the Top of a Rayleigh Atmosphere", Sci. Rep. No. 1, Dept. of Meteor., Univ. of California at Los Angeles.

Coulson, K. L., Dave, J. V. and Sekera, Z. (1960), Tables Related to the Radiation Emerging from a Planetary Atmosphere with Rayleigh Scattering, Univ. of California Press, Berkeley and Los Angeles.

Danilov, A. D. (1961), Geomagnetizm i aeronomiya 1, 45.

Diermendjian, D. (1955), "Optical Thickness of a Molecular Atmosphere", Archiv. Meteor., Geophys. u. Bioklim, Ser. B, 6, 452.

Diermendjian, D. and Vestine, E. H. (1959), "Some Remarks on the Nature and Origin of Noctilucent Cloud Particles", Planet. Space Sci. 1, 146.

Fishkova, L. M. and Markova, G. V. (1960), "Certain Results of Electrophotometric and Spectrographic Observations of Night Airglow in Abastumani", Spectral, Electrophotometrical, and Radar Researches of Aurora and Airglow, No. 2-3, 51.

Glenn, Jr., J. H. (1962), "Pilot's Flight Report", in Results of First United States Orbital Flight, NASA. Manned Spacecraft Center. U. S. Govt. Printing Office, Washington, D. C.

Grishin, N. I. (1956), All-Union Astr. Geod. Soc. Bull. 19, 3.

Hesstvedt, E. (1961), "Note on the Nature of Noctilucent Clouds", J. Geophys. Res. 66, 1985.

Hoffmeister, C. (1961), Ann. of IGY 11.

Ludham, F. H. (1957), "Noctilucent Clouds", Tellus 9, 341.

Mikirov, A. E. (May, 1962), "Aerosole Scattering Coefficient Measurement at the 80-100 km Altitude", COSPAR, Third International Space Science Symposium.

Mirtov, B. A. (1962), "Meteoric Matter and Some Geophysical Problem of the Upper Atmosphere", ARS J. 32, 143.

Naqvi, A. M. (1962), "Satellite Navigation by Terrestrial Occultations of Stars I: General Considerations Neglecting Atmospheric Refraction and Extinction", GCA Tech. Report 62-18-A.

Naqvi, A. M. (1962), "Satellite Navigation by Terrestrial Occultations of Stars II: Considerations Relating to Refraction and Extinction", GCA Tech. Report 62-21-A.

O'Keefe, J. A. (1962), in "Results of the Second Manned Orbital Space Flight", NASA, Space Science Report 6.

Packer, D. M. (1961), "Altitudes of the Night Airglow Radiations", Ann. de geophysique 17, 67.

Sharonov, V. V. (1960), "Photometric Conditions of Noctilucent Cloud Visibility", Translation distributed by Office of Technical Services, Mezhdunarodnyy Geofizicheskiy God. Sbornik stately i materialov, 12.

Wallace, L. J. (1961), "An Attempt to Observe the Day Airglow", J. Geophys. Res. 66, 1585.

Witt, G. (1960), "Polarization of Light from Noctilucent Clouds", J. Geophys. Res. 65, 925.